

# Energy dissipation of electrons at a *p*-type GaAs(110) surface

Hiroshi Imada,<sup>1</sup> Kuniyuki Miwa,<sup>1</sup> Jaehoon Jung,<sup>1</sup> Tomoko K. Shimizu,<sup>1,\*</sup> Naoki Yamamoto,<sup>2</sup> and Yousoo Kim<sup>1,†</sup>

<sup>1</sup>*Surface and Interface Science Laboratory, RIKEN, 2-1 Hirosawa, Wako, Saitama 351-0198, Japan*

<sup>2</sup>*Department of Condensed Matter Physics, Tokyo Institute of Technology,*

*2-12-1 Oh-okayama, Meguro, Tokyo 152-8551, Japan*

(Dated: June 2, 2021)

Electron injection from the tip of a scanning tunneling microscope into a *p*-type GaAs(110) surface have been used to induce luminescence in the bulk. Atomically-resolved photon maps revealed significant reduction of the luminescence intensity at surface states localized near Ga atoms. Quantitative analysis based on the first principles calculation and a rate equation approach was performed to describe overall energy dissipation processes of the incident tunneling electrons. Our study shows that the recombination processes in the bulk electronic states are suppressed by the fast electron scattering at the surface, and the electrons dominantly undergo non-radiative recombination through the surface states.

PACS numbers: 68.37.Ef, 68.47.Fg, 73.20.At, 78.55.Cr, 78.68.+m

Energy dissipation processes of electrons such as recombination and scattering play significant roles in current electronic technologies. In particular, recombination at surfaces is one of the principal processes responsible for reducing the operational efficiency of (opto)electronic devices and (photo)catalytic systems [1–4]. Recent development of wide varieties of nano-materials further raises the importance to precisely understand recombination at surfaces, because such materials have large surface-to-volume ratios [3–5]. However, it has so far not been feasible to obtain quantitative information about surface recombination at the atomic-scale, mainly because of technical limitations (*vide infra*).

Investigation of surface recombination requires selective excitation of surface electronic states. In cathodoluminescence and photoluminescence (PL), which have been widely used to study recombination processes in semiconductor materials [6], the fact that the electronic excitation occurs mainly inside the bulk hampers investigation of surface phenomena. Two-photon photoemission (2PPE) has been applied to the study of electron dynamics at various semiconductor surfaces [7–9], but 2PPE has a restriction in obtaining detailed spatial information. In contrast, scanning tunneling luminescence (STL) [10–13], where luminescence is induced by tunneling electrons from the tip of a scanning tunneling microscope (STM), has several distinctive capabilities. Selective and direct excitation of surfaces can be achieved by the injection of energetic electrons into surface electronic states in STL, and its ability to spatially resolve materials at atomic resolution makes it unique among optical techniques. In conjunction with morphological observation with an STM and electronic state measurement using scanning tunneling spectroscopy (STS), STL is an ideal tool for investigating surface recombination.

GaAs, a III-V compound semiconductor, is one of the most important industrial materials used in optoelectronic devices such as photovoltaic cells and

lasers. The electronic properties of the GaAs(110) surface have been intensively studied using photo-electron spectroscopy [7], theoretical calculations [14–16], and STM [15–25]. GaAs(110) has also been studied with STL, focusing mainly on understanding the mechanism of the luminescence induced by STM, including electron tunneling, electronic transitions, and electromagnetic enhancement [10, 26–30]. However, STL has never been used to investigate the surface recombination at a GaAs(110) surface, and so far detailed features of energy dissipation at the surface are veiled.

In this Letter, we report on the investigation of the mechanism responsible for energy dissipation at a *p*-type GaAs(110) surface studied using STL spectroscopy. Luminescence from the bulk GaAs was measured by varying the location of electron-injection, and atomically-resolved photon maps showed significant reduction of the luminescence intensity at surface states localized near Ga atoms. Theoretical analysis using the first principles calculation and a rate equation approach revealed that the injected tunneling electrons dominantly undergo non-radiative recombination through the surface state, and other recombination processes, *i.e.* radiative and non-radiative recombination in the bulk electronic states, are suppressed by the fast electron scattering at the surface.

Experiments were performed with a low-temperature STM (Omicron) operating at 4.7 K under ultrahigh vacuum (UHV). The STM stage is equipped with two optical lenses. The emitted light was collimated and led outside the UHV chamber with a lens and refocused into a spectrometer (Acton, SpectraPro 2300i) with a photon detector (Princeton, Spec-10). In the STL measurement except for the luminescence spectrum, integrated photon intensity over a wavelength range of 750–1000 nm is plotted. The sample was *p*-type GaAs heavily doped with Zn at a carrier concentration of around  $2 \times 10^{19} \text{ cm}^{-3}$ , and cleaved under UHV to expose clean (110) surfaces. The STM tip was prepared by electrochemical etching of a

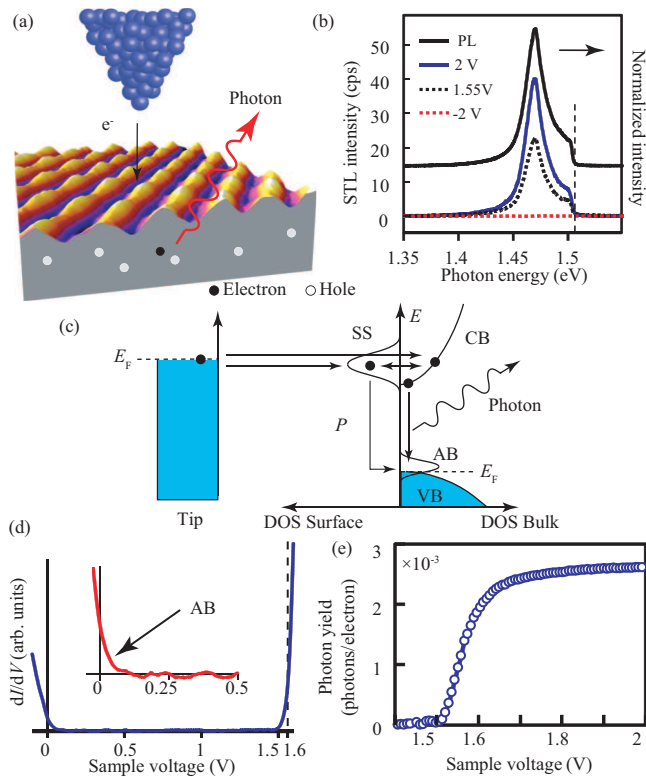


FIG. 1. (Color online) (a) Schematic representation of STL measurement of *p*-doped GaAs. Luminescence inside the bulk is induced by electron injection with an STM tip. (b) STL spectra at various voltages and a PL spectrum measured on the same sample. All STL spectra were acquired with a tunneling current ( $I_t$ ) of 100 pA and an exposure time of 1 min., and the intensity was measured in counts per second (cps). The PL spectrum is normalized and offset. The PL was excited by a green laser (532 nm, 1 mW). (c) Schematic energy diagram illustrating the proposed process (described in the main text).  $E_F$ : Fermi level. (d)  $dI/dV$  curve measured on GaAs(110). The region near the VB maximum is shown in the inset. (e) Sample voltage dependence of the photon yield. Photon yield = (number of emitted photons)/(number of injected electrons).

tungsten wire.

First principles calculations based on density functional theory (DFT) were performed to analyze the electronic structure of GaAs(110) surface. We employed the local density approximation [31] implemented in the Vienna *ab initio* simulation package code [32, 33]. The core electrons were replaced by projector augmented wave pseudopotentials and expanded in a plan-wave basis set (480 eV cutoff) [34, 35]. The repeated slab model consists of 17 atomic (110) planes separated by a vacuum region of more than 15 Å, in which bottom atoms were terminated with hydrogen. Dipole correction was applied in order to avoid artificial interactions between periodic slab images. During ionic relaxations, the two bottom atomic (110) planes were fixed in their bulk positions. Ionic relaxations were performed until atomic forces became less

than 0.01 eV/Å. A  $12 \times 16 \times 1$   $\Gamma$ -centered  $k$ -point grid was used for Brillouin zone sampling.

In the STL experiments, luminescence of *p*-type GaAs induced by the STM was measured and correlated with local atomic and electronic structures (Fig. 1(a)). Figure 1(b) shows STL spectra of the GaAs(110) measured at various sample voltages ( $V$ ) and a PL spectrum as a reference. Luminescence in STL was observed only at positive  $V$  when  $|V|$  is less than two volts [26]. The shape of STL spectra (a single peak at 1.47 eV and a cutoff at 1.51 eV) did not depend on  $V$ , and it was almost identical to that of the PL spectrum, suggesting that no radiative recombination occurs at the surface. Because the excitation light in PL penetrates about 100 nm into GaAs [36], the luminescence occurs mainly inside the bulk. Therefore, we concluded that STL also occurs inside the bulk.

A proposed process of the STL is summarized in Fig. 1(c). First, electrons tunnel from the tip into surface states (SS) or the conduction band (CB). While the electrons are in SS, they may undergo surface non-radiative recombination with a certain probability  $P$ . Electrons that do not undergo the non-radiative recombination at the surface penetrate into the bulk CB, followed by thermalization to the CB minimum. They then recombine with holes in the acceptor band (AB) just above the Fermi level giving rise to luminescence [6, 27]. The abrupt cutoff observed at 1.51 eV in the spectrum suggests that the highest-energy transition is from the CB minimum to the Fermi level, which indicates that the AB merges with the intrinsic valence band (VB) [6, 37]. In other words, the sample is degenerate. Figure 1(d), which shows the density of state of GaAs(110) measured with STS, confirms the existence of the empty state associated with the AB (indicated by an arrow in the inset of Fig. 1(d)) [38].

The dependence of photon yield on sample voltage ( $V$ ) is shown in Fig. 1(e). The yield exhibits a rapid rise at 1.51 V, and the slope starts to decrease at 1.6 V, followed by saturation at around 1.8 V. This behavior reflects the ratio of the number of electrons injected into the bulk CB to the total number of tunneling electrons. When  $V$  is lower than 1.51 V, the only state available for tunneling should be the empty AB. Once the bias voltage exceeds 1.51 V, the tunneling channel into the bulk CB opens up. The proportion of electrons tunneling into the bulk CB, which induces the luminescence, then begins to increase with increasing  $V$ . Because the internal quantum efficiency of the luminescence inside the bulk is on the order of  $10^{-1}$  [37, 39], the observed low saturation value of the photon yield ( $2.5 \times 10^{-3}$ ), though this is slightly larger than the previously reported values [26, 28], cannot be explained without consideration of the surface electronic states which promote non-radiative recombination at the surface. To elucidate the role of the surface electronic states in non-radiative recombination at the surface, we obtained STL photon maps at atomic resolution and ex-

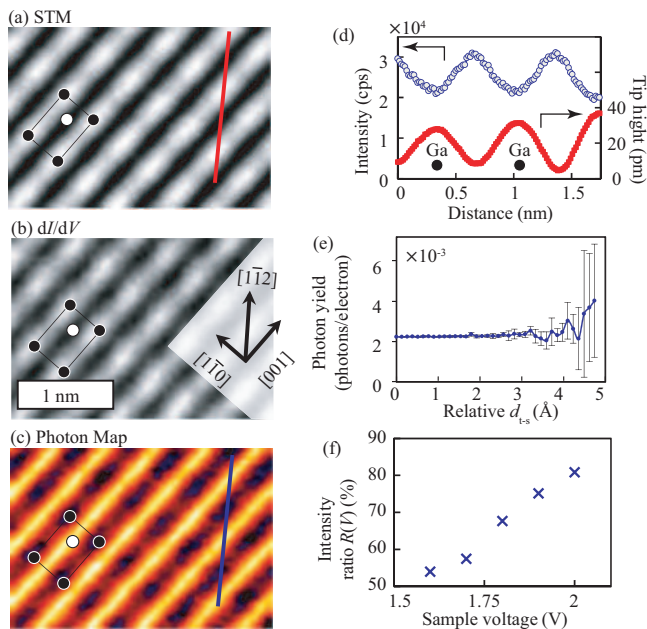


FIG. 2. (Color online) (a) An atomically resolved STM image, (b) a  $dI/dV$  map and (c) an STL photon map of GaAs(110) ( $V = 1.8$  V). A unit cell at identical positions is shown (black: Ga, white: As). (d) Line profiles of an STM image and STL photon map ( $V = 1.6$  V,  $I_t = 100$  pA) along the  $[1\bar{1}2]$  direction, as indicated by the lines in (a) and (c), respectively. (e) Tip-sample distance dependence of the photon yield. Tunneling current and photon intensity were simultaneously measured while the tip was gradually retracted away from the initial tip-sample distance. The photon yield was calculated from the observed number of photon and the number of injected electrons at each  $d_{t-s}$ . Tip-sample distance is measured from the initial distance which is determined by the tunneling condition of  $V = 1.8$  V,  $I_t = 100$  pA. (f) Ratio of photon intensity at the Ga site with respect to that at the center of unit cell plotted against sample voltage.

amined the correlation of the photon intensity distribution with the underlying atomic configuration.

An atomically resolved STM image,  $dI/dV$  map, and STL photon map measured at  $V = 1.8$  V are shown in Figures 2(a)-(c). The atomic rows in the STM and  $dI/dV$  images apparently run in the  $[001]$  direction, similar images were obtained in the voltage range of 1.6-2.0 V. The bright spots in an STM image observed within the voltage range correspond to the surface Ga atoms [15, 16]. In the same voltage range, STL photon maps show similar stripe-like patterns running in the  $[001]$  direction. However, in contrast to the STM image and the  $dI/dV$  map, dark spots were observed at Ga sites in the photon map. The correlation between the contrasts of an STM image and a photon map can be seen more clearly with line profiles in Fig. 2(d). A similar observation showing an almost-inverted correlation of an STM image with a photon map has been reported on Au(110), where the contrast inversion was explained by tip-induced plasmon

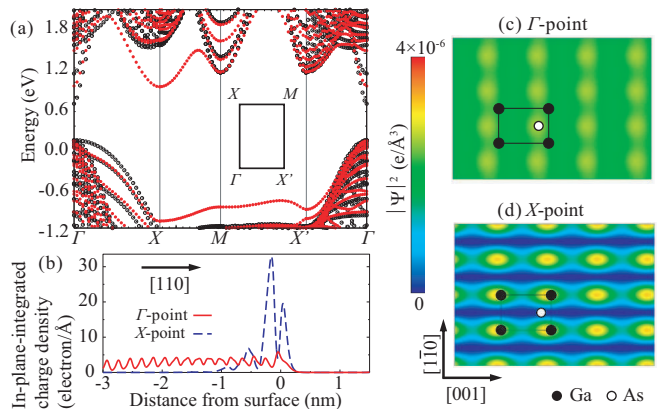


FIG. 3. (Color online) (a) Band structure for GaAs(110) surface (red) and projected bulk band structure (black). Inset shows the surface Brillouin zone. (b)  $|\Psi|^2$  integrated in planes parallel to the surface were plotted as a function of the distance from the surface. (c), (d)  $|\Psi|^2$  in a  $(110)$  plane at 4 Å above the surface As atom. The similar value of  $z$  has been typically used for analyzing the distribution of surface electron density [16, 40]. Charge densities were visualized using VESTA software [41].

effects based on the change in electromagnetic interaction between the STM tip and the metallic sample as a function of the tip-sample distance ( $d_{t-s}$ ) [12]. To examine the influence of the plasmon effect, we measured the photon yield as a function of  $d_{t-s}$  (Fig. 2(e)), which shows that the photon yield is fairly constant, at least for  $d_{t-s} < 2.5$  Å. The contrast in the STL photon maps therefore arises from surface non-radiative recombination without any influence from the tip-induced plasmon effect.

Local variation of the photon intensity in STL (Fig. 3(c)) can be analyzed by considering local electron-injection into the electronic states distributed on the GaAs(110) surface and dynamic processes of the electrons at the surface. In order to identify the electronic states responsible for the tunneling, we investigated the electronic structure of GaAs(110) using DFT calculations. Figure 3(a) shows the band structure of the GaAs(110) surface, in which the bulk band structure is also projected for comparison. The first unoccupied surface band ( $C_3$  band) has valleys at the  $\Gamma$ - and  $X$ -points of the surface Brillouin zone; although the bottoms of these valleys are located at almost identical energy levels, the  $C_3$  band is resonant with the bulk CB only at  $\Gamma$ , and it lies within the energy gap of the projected bulk band at  $X$ . Because other valleys in the  $C_3$  band and the upper unoccupied surface bands are located higher in energy, tunneling electrons would be dominantly injected into the  $\Gamma$ - and  $X$ -valleys of the  $C_3$  band, when the sample voltage is slightly above the band gap.

Figures 3(b)-(d) show spatial distribution of charge densities ( $|\Psi_{1,\Gamma}|^2$  and  $|\Psi_{1,X}|^2$ ) of the  $C_3$  band at  $\Gamma$  and

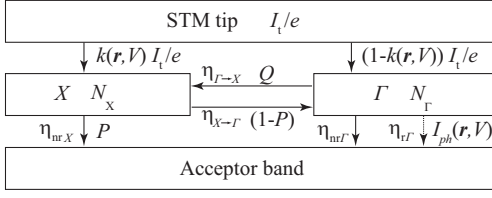


FIG. 4. A schematic of the energy dissipation model. All parameters are defined in the main text.

$X$ , i.e.  $|1, \Gamma\rangle$  and  $|1, X\rangle$ , respectively. Figure 3(b) clearly displays that  $|\Psi_{1, \Gamma}|^2$  penetrates into the bulk whereas  $|\Psi_{1, X}|^2$  is localized at the surface. Figure 3(c) shows a relatively uniform distribution of  $|\Psi_{1, \Gamma}|^2$  on the surface. In contrast,  $|\Psi_{1, X}|^2$  is strongly localized around the surface Ga atoms (Fig. 3(d)), which has a large value at the Ga sites and it becomes very small at the center of the unit cell. It is clear that when the STM tip is located above the surface Ga atoms  $|1, X\rangle$  mainly contributes to the tunneling, whereas contribution from  $|1, \Gamma\rangle$  is dominant when the tip is located above the center of the unit cell.

As a next step, we consider dynamics of the electrons injected into the surface states (a schematic of the model is illustrated in Fig. 4) using a rate equation approach. We assume that electrons are injected into either  $|1, \Gamma\rangle$  or  $|1, X\rangle$ , because the DFT calculation shows that the contributions from other states are negligible in our experimental condition. Rate equations regarding the number of electron  $N_\Gamma$  and  $N_X$  in  $|1, \Gamma\rangle$  and  $|1, X\rangle$ , respectively, are given by

$$\frac{dN_\Gamma}{dt} = (1 - k(\mathbf{r}, V)) \frac{I_t}{e} - (\eta_{r\Gamma} + \eta_{nr\Gamma} + \eta_{\Gamma \rightarrow X}) N_\Gamma + \eta_{X \rightarrow \Gamma} N_X, \quad (1)$$

$$\frac{dN_X}{dt} = k(\mathbf{r}, V) \frac{I_t}{e} - (\eta_{nrX} + \eta_{X \rightarrow \Gamma}) N_X + \eta_{\Gamma \rightarrow X} N_\Gamma, \quad (2)$$

when the ratio of the tunneling current injected into  $|1, X\rangle$  to the total tunneling current  $I_t$  is defined as  $k(\mathbf{r}, V)$ , which is a function of STM tip position  $\mathbf{r}$  and sample voltage  $V$ .  $\eta_{ri}$  and  $\eta_{nri}$  are radiative and non-radiative recombination rates in  $i$  ( $i = \Gamma, X$ ), respectively.  $\eta_{\Gamma \rightarrow X}$  and  $\eta_{X \rightarrow \Gamma}$  are transfer rates of  $\Gamma \rightarrow X$  and  $X \rightarrow \Gamma$  intervalley scattering processes [7], and  $e$  is the element charge. We considered the radiative recombination only at  $\Gamma$ , because the band structure is indirect at  $X$ . In a steady state, photon intensity induced by the tunneling current is expressed as

$$I_{ph}(\mathbf{r}, V) = Y \frac{(1 - Q)(1 - Pk(\mathbf{r}, V)) I_t}{1 - Q(1 - P)} \frac{I_t}{e}, \quad (3)$$

where  $Y \equiv \eta_{r\Gamma}/(\eta_{r\Gamma} + \eta_{nr\Gamma})$  is the internal quantum efficiency of the luminescence in the bulk,  $Q \equiv \eta_{\Gamma \rightarrow X}/(\eta_{r\Gamma} +$

$\eta_{nr\Gamma} + \eta_{\Gamma \rightarrow X})$  is the probability of  $\Gamma \rightarrow X$  intervalley scattering, and  $P \equiv \eta_{nrX}/(\eta_{nrX} + \eta_{X \rightarrow \Gamma})$  is the probability of non-radiative surface recombination. Although we have not yet reached a conclusion concerning the dominant process for the surface non-radiative recombination, Auger and Shockley-Hall-Read (SHR) processes are likely to contribute because the doping level of our sample is relatively high and unavoidable defects such as vacancies and atomic steps have been observed on the surface.

If we take a ratio of two photon intensities,  $Y$  and  $Q$  are eliminated from the equation (3) and  $P$  can be estimated from the experimental results. We define a quantity  $R(V)$ , which is the ratio of photon intensities measured with the tip position above the surface Ga atom and above the center of the unit cell (data shown in Fig. 2(f)),

$$R(V) \equiv \frac{I_{ph}(\text{Ga}, V)}{I_{ph}(\text{center}, V)} = \frac{1 - Pk(\text{Ga}, V)}{1 - Pk(\text{center}, V)}. \quad (4)$$

Because  $|\Psi_{1, X}|^2$  at the Ga site is much larger than that at the center of the unit cell (Fig. 3(d)), we can assume  $0 \leq k(\text{center}, V) \leq k(\text{Ga}, V) \leq 1$ , thus the following relationship is obtained:

$$1 - R(V) \leq P. \quad (5)$$

The minimum value of  $R$  observed in the experiment is 54% at 1.6 V (Fig. 2(f)). Therefore we concluded that the non-radiative recombination probability  $P$  for electrons in  $|1, X\rangle$  is at least 46%.

$P$  and  $Q$  were also estimated in another way by solving simultaneous equations. Using the formula (3), two independent equations were obtained for the photon intensities at the two tip positions,  $I_{ph}(\text{Ga}, V)$  and  $I_{ph}(\text{center}, V)$ . We adopted the reported value of  $Y \approx 0.24$  for Zn-doped GaAs with the carrier concentration of  $2 \times 10^{19} \text{ cm}^{-3}$  [37], and the values of  $k(\text{Ga}, V)$  and  $k(\text{center}, V)$  were approximately estimated to be 0.63 and 0, respectively, from the result of DFT calculation (Fig. 3(c), (d)). Estimated  $P$  value is 53%, which satisfies the experimentally determined relationship  $P \geq 48\%$ . In addition, we found a very large value for  $Q$ , 99.99%, i.e. very high probability of  $\Gamma \rightarrow X$  intervalley scattering. It can be explained by the short transfer time  $\tau_{\Gamma \rightarrow X} = 1/\eta_{\Gamma \rightarrow X} \approx 0.4 \text{ psec}$  [7], which is about 1000 times shorter than the recombination lifetime of  $\sim \text{ns}$  in the bulk GaAs [39].

In conclusion, we unveiled the energy dissipation mechanism of electrons at the  $p$ -type GaAs(110) surface based on the atomically-resolved STL observation and the theoretical analysis. The probability of non-radiative recombination for electrons in the  $X$ -valley of the  $C_3$  band was estimated to be around 50%, which is not high enough to explain the low luminescence yield of  $\sim 10^{-3}$  in the STL of GaAs(110). The key process is the fast  $\Gamma \rightarrow X$  intervalley scattering that prevents the injected electrons

from penetrating into the bulk [7], and it scatters electrons escaped from  $X$  to  $\Gamma$  immediately back into  $X$  with a very high probability. Eventually the vast majority of the injected electrons undergo the non-radiative recombination at the surface after several cycles of  $\Gamma \rightleftharpoons X$  intervalley scatterings, which suppresses the luminescence in the bulk.

This work was financially supported in part by a Grant-in-Aid for Scientific Research (S) “Single Molecule Spectroscopy Using Probe Microscope” [21225001] from the Ministry of Education, Culture, Sports, Science and Technology (MEXT) of Japan. We thank David W. Chapmon for carefully reading the manuscript and Ryuichi Arafune for helpful discussion.

---

\* Current address: National Institute for Materials Science, 1-2-1 Sengen, Tsukuba, Ibaraki, 305-0047, Japan

† Correspondence should be addressed to Y. K. at: ykim@riken.jp

- [1] C. H. Henry, R. A. Logan, and F. R. Merritt, *J. Appl. Phys.* **49**, 3530 (1978).
- [2] O. A. Semenikhin, V. E. Kazarinov, L. Jiang, K. Hashimoto, and A. Fujishima, *Langmuir* **15**, 3731 (1999).
- [3] J. E. Allen *et al.*, *Nat. Nanotechnol.* **3**, 168 (2008).
- [4] Y. Dan, K. Seo, K. Takei, J. H. Meza, A. Javey, and K. B. Crozier, *Nano Lett.* **11**, 2527 (2011).
- [5] X. Chen and S. S. Mao, *Chem. Rev.* **107**, 2891 (2007).
- [6] J. I. Pankove, *Optical processes in semiconductors* (Dover, New York, 1971).
- [7] R. Haight and J. A. Silberman, *Phys. Rev. Lett.* **62**, 815 (1989).
- [8] J. Bokor, R. Haight, R. H. Storz, J. Stark, R. R. Freeman, and P. H. Bucksbaum, *Phys. Rev. B* **32**, 3669 (1985).
- [9] N. J. Halas and J. Bokor, *Phys. Rev. Lett.* **62**, 1679 (1989).
- [10] M. Reinhardt, G. Schull, P. Ebert, and R. Berndt, *Appl. Phys. Lett.* **96**, 152107 (2010).
- [11] H. Imada, M. Ohta, and N. Yamamoto, *Appl. Phys. Express* **3**, 045701 (2010).
- [12] R. Berndt, R. Gaisch, W. D. Schneider, J. K. Gimzewski, B. Reihl, R. R. Schlittler, and M. Tschudy, *Phys. Rev. Lett.* **74**, 102 (1995).
- [13] A. Downes and M. E. Welland, *Phys. Rev. Lett.* **81**, 1857 (1998).
- [14] J. R. Chelikowsky and M. L. Cohen, *Phys. Rev. B* **20**, 4150 (1979).
- [15] B. Engels, P. Richard, K. Schroeder, S. Blugel, P. Ebert, and K. Urban, *Phys. Rev. B* **58**, 7799 (1998).
- [16] P. Ebert, B. Engels, K. Richard, P. and Schroeder, S. Blugel, C. Domke, M. Heinrich, and K. Urban, *Phys. Rev. Lett.* **77**, 2997 (1996).
- [17] S. Loth, M. Wenderoth, R. G. Ulbrich, S. Malzer, and G. H. Dohler, *Phys. Rev. B* **76**, 235318 (2007).
- [18] R. de Kort, M. C. M. M. van der Wielen, A. J. A. van Roij, W. Kets, and H. van Kempen, *Phys. Rev. B* **63**, 125336 (2001).
- [19] Z. F. Zheng, M. B. Salmeron, and E. R. Weber, *Appl. Phys. Lett.* **64**, 1836 (1994).
- [20] S. Loth, M. Wenderoth, L. Winking, R. G. Ulbrich, S. Malzer, and G. H. Dohler, *Phys. Rev. Lett.* **96**, 066403 (2006).
- [21] G. Mahieu, B. Grandidier, D. Deresmes, J. P. Nys, D. Stiévenard, and P. Ebert, *Phys. Rev. Lett.* **94**, 026407 (2005).
- [22] S. Yoshida, Y. Kanitani, O. Takeuchi, and H. Shigekawa, *Appl. Phys. Lett.* **92**, 102105 (2008).
- [23] D. H. Lee, N. M. Santagata, and J. A. Gupta, *Appl. Phys. Lett.* **99**, 053124 (2011).
- [24] A. Richardella, D. Kitchen, and A. Yazdani, *Phys. Rev. B* **80**, 045318 (2009).
- [25] G. Münnich, A. Donarini, M. Wenderoth, and J. Repp, *Phys. Rev. Lett.* **111**, 216802 (2013).
- [26] T. Yokoyama and Y. Takiguchi, *Surf. Sci.* **482-485**, 1163 (2001).
- [27] M. Hoshino and N. Yamamoto, *MRS Symposium Proceedings* **738**, 149 (2002).
- [28] D. Fujita, K. Onishi, and N. Niori, *Nanotechnology* **15**, S355 (2004).
- [29] Y. Uehara, H. Gotoh, R. Arafune, and S. Ushioda, *J. Appl. Phys.* **93**, 3784 (2003).
- [30] X. L. Guo, D. Fujita, N. Niori, K. Sagisaka, and K. Onishi, *Nanotechnology* **18**, 195201 (2007).
- [31] J. Perdew and A. Zunger, *Phys. Rev. B* **23**, 5048 (1981).
- [32] G. Kresse and J. Furthmüller, *Phys. Rev. B* **54**, 11169 (1996).
- [33] G. Kresse and J. Furthmüller, *Comput. Mater. Sci.* **6**, 15 (1996).
- [34] P. E. Blöchl, *Phys. Rev. B* **50**, 17953 (1994).
- [35] G. Kresse and D. Joubert, *Phys. Rev. B* **59**, 1758 (1999).
- [36] D. E. Aspnes and A. A. Studna, *Phys. Rev. B* **27**, 985 (1983).
- [37] D. A. Cusano, *Solid State Commun.* **2**, 353 (1964).
- [38] V. Fiorentini, *Phys. Rev. B* **51**, 10161 (1995).
- [39] R. J. Nelson and R. G. Sobers, *J. Appl. Phys.* **49**, 6103 (1978).
- [40] J. Wang, T. A. Arias, J. D. Joannopoulos, G. W. Turner, and O. L. Alerhand, *Phys. Rev. B* **47**, 10326 (1993).
- [41] K. Momma and F. Izumi, *J. Appl. Crystallogr.* **44**, 1272 (2011).